

1 **Effects of aspalathin on insulin resistance and mitochondrial dysfunction in cultured skeletal muscle cells -**
2 **potential implications for type 2 diabetes mellitus therapy**

3 Sithandiwe E. Mazibuko-Mbeje¹, Sinenhlanhla X.H. Mthembu^{1,2}, Christo J.F. Muller^{2,3,4}, Khanyisani Ziqubu ¹,
4 Ndivhuwo Muvhulawa¹, Reneilwe V. Modibedi¹, Luca Tiano⁵, Phiwayinkosi V. Dlodla²

5 ¹Department of Biochemistry, North-West University, Mafikeng Campus, Mmabatho 2735, South Africa.

6 ²Biomedical Research and Innovation Platform, South African Medical Research Council, Tygerberg 7505, South
7 Africa.

8 ³Division of Medical Physiology, Stellenbosch University, Tygerberg 7505, South Africa.

9 ⁴Department of Biochemistry and Microbiology, University of Zululand, KwaDlangezwa 3886, South Africa.

10 ⁵Department of Life and Environmental Sciences, Polytechnic University of Marche, Ancona 60131, Italy.

11

12 Correspondence:

13 Professor Sithandiwe E. Mazibuko-Mbeje, PhD

14 Department of Biochemistry, Faculty of Natural and Agricultural Sciences, North-West University, Mafikeng
15 Campus, Private Bag X 2046, Mmabatho 2735, South Africa. Email: 36588296@nwu.ac.za. Tel.:018 399 2354

16

17

18 **Abstract**

19 Natural compounds may bare promising therapeutic benefits against metabolic diseases such as type 2 diabetes
20 mellitus (T2DM), which are characterized by a state of insulin resistance and mitochondrial dysfunction. Here,
21 we examined the cellular mechanisms by which aspalathin, a dihydrochalcone C-glucoside unique to rooibos,
22 may ameliorate palmitate-induced insulin resistance and mitochondrial dysfunction in cultured C2C12
23 myotubules. This current study demonstrated that aspalathin remains effective in improving glucose uptake in
24 insulin-resistant skeletal muscle cells, supported by the upregulation of insulin-dependent signaling that involves
25 the activation of insulin receptor (IR) and direct phosphorylation of protein kinase B (AKT). Interestingly,
26 aspalathin also improved mitochondrial respiration and function, which was evident by an increased expression
27 of carnitine palmitoyltransferase 1 (*Cpt1*), fatty acid transport protein 1 (*Fatp1*), sirtuin 1 (*Sirt1*), nuclear
28 respiratory factor 1 (*Nrf1*), and transcription factor A, mitochondrial (*Tfam*). Importantly, our results showed
29 that aspalathin treatment was effective in ameliorating the devastating outcomes of insulin resistance and
30 mitochondrial dysfunction that are linked with an undesired pro-inflammatory response, by reducing the levels
31 of well-known pro-inflammatory markers such as interleukin-6 (*IL-6*), tumor necrosis factor-alpha (*TNF-α*), and
32 protein kinase C-theta (PKC-θ). Thus, beyond improving glucose uptake and insulin signaling, the current study
33 brings a new perspective in the therapeutic benefits of aspalathin in improving mitochondrial respiration and
34 blocking inflammation to attenuate the detrimental effect of palmitate in skeletal muscle cells.

35

36 **Keywords:**

37 Type 2 diabetes mellitus; skeletal muscle insulin resistance; aspalathin; insulin signaling; mitochondrial
38 dysfunction and inflammation.

39

40 1. Introduction

41 The rapid increase in the prevalence of diabetes mellitus, particularly type 2 diabetes mellitus (T2DM) [1] is of
42 major concern, due to its significant contribution to the overall increase in global deaths [2]. Modifiable risk
43 factors such as excessive nutrient intake, which are usually coupled with a sedentary lifestyle, are acknowledged
44 to be the main instigators in the development of diverse metabolic diseases including T2DM [3]. In fact, excessive
45 body fat accumulation in a state of obesity is responsible for the development of insulin resistance, a major
46 characteristic feature of T2DM [3]. Indeed, impairments in insulin signaling, mainly accompanied by suppressed
47 muscle glucose homeostasis or derangements in free fatty acid oxidation within the skeletal muscle are
48 recognized as established pathological mechanisms unique to T2DM [4]. This also explains the significance of
49 the skeletal muscle in maintaining essential physiological processes, especially its role in regulating energy
50 metabolism, including the uptake and utilization of major substrates like glucose and free fatty acids [5].

51 Notably, well-known interventions like physical activity are acknowledged to alleviate some metabolic
52 complications by improving skeletal muscle glucose utilization, or even by modulating molecular mechanisms
53 involved in energy metabolism and insulin signaling [6, 7]. Regarding the latter, prime examples include effective
54 regulation of insulin-dependent mechanisms like the phosphoinositide 3-kinase (PI3K)/protein kinase B (AKT)
55 pathway. Briefly, through binding to the insulin receptor (IR), insulin can directly stimulate PI3K, which leads to
56 the activation of protein kinases such as AKT that promote glucose uptake within the skeletal muscle [8].
57 Interestingly, accumulative research has indicated that diverse pharmacological compounds, including
58 established antidiabetic drugs like insulin and metformin, mainly function through activation of such molecular
59 mechanisms to reverse insulin resistance or alleviate complications linked with T2DM [9-11].

60 Likewise, available research has indicated that herbal medicine has the potential to ameliorate metabolic
61 abnormalities linked with insulin resistance by improving insulin sensitivity, in part through effective regulation
62 of PI3K/AKT pathways [12-14]. Particular interest has also been placed on characterizing and determining the
63 relative levels of bioactive compounds found in herbal medicines, as the major therapeutic effects of these
64 plants are attributed to these exceptional compounds. In fact, due to its envisaged health capabilities, there has
65 been a general interest in understanding the therapeutic potential of bioactive compounds found in rooibos
66 (*Aspalathus linearis*) in ameliorating metabolic diseases and improving human health [15-19]. As such, our
67 research group has progressively explored the ameliorative effects of aspalathin, the major dihydrochalcone
68 unique to rooibos, against metabolic complications linked with insulin resistance and T2DM in various preclinical
69 models. Available evidence suggests that beyond controlling substrate metabolism, including regulating the
70 utilization of glucose and free fatty acids [20-22], aspalathin or extracts rich in this bioactive compound can
71 modulate essential cellular mechanisms involved in cell survival, such as the PI3K/AKT signaling, mitochondrial
72 respiration, and even autophagy to hinder cellular damage in various experimental models of diabetes [23-28].
73 Notably, there is not much information that has been reported on the direct impact of aspalathin in salvaging
74 palmitate-induced insulin resistance, mitochondrial dysfunction, or suppressing pro-inflammatory markers in
75 cultured C2C12 myotubes. Thus, beyond enhancing our current understanding of the therapeutic effects of

76 aspalathin, the current study completes a global perspective on the link between insulin resistance and
77 mitochondrial dysfunction. Lastly this study also demonstrated the potential protective effect of aspalathin has
78 gained palmitate induce inflammation, which is also known as risk factor of T2DM.

79

80 **2. Materials and methods**

81 **2.1. Reagents**

82 Murine C2C12 skeletal muscle cells (Catalog No. CRL-1772) were obtained from the American Type Culture
83 Collection (Manassas, VA, USA). Aspalathin ($\geq 98\%$ purity, batch SZ1-356-54) was acquired from High Force
84 Research LTD (Durham, UK). Dulbecco's Modified Eagle's Medium (DMEM), Dulbecco's phosphate-buffered
85 saline (DPBS, pH 7.4 with calcium and magnesium), penicillin-streptomycin and luminescent ATP kit were
86 obtained from Lonza (Walkersville, MD, USA). Horse serum (HS) and fetal calf serum (FCS) were from Biochrom
87 (Berlin, Germany), and PrestoBlue™ cell viability reagent was purchased from Invitrogen (Karlsruhe, Germany).
88 2-Deoxy-[³H]-D-glucose was from American Radiolabelled Chemicals (St Louis, MO, USA). Bradford protein assay
89 kits were from Bio-Rad Laboratories (Hercules, CA, USA). Cell Signalling Technology (Beverly, MA, USA) supplied
90 primary antibodies, including protein kinase C-theta (PKC θ), p/PKC θ ^(Ser 643/676), protein kinase B (AKT), p-AKT
91 (Ser473) (Ser ⁴⁷³), as well as insulin receptor (IR). The reference control, beta (β)-actin, and the secondary
92 antibodies; goat-anti-mouse and goat-anti rabbit IgG – horseradish peroxidase (HRP) were purchased from Santa
93 Cruz Biotechnology (Dallas, TX, USA). Quant-iT™ PicoGreen™ dsDNA quantitation assay kits, TRIzol reagent,
94 Turbo DNase Kit, and all PCR probes were supplied by ThermoFisher Scientific, Inc. (Waltham, MA, USA). Taqman
95 Master Mix, QIAzol, QuantiTect Reverse Transcription Kit were obtained from Qiagen (Valencia, CA, USA).
96 Reagents for Seahorse experiments such as oligomycin, carbonyl cyanide p-trifluoromethoxyphenylhydrazone
97 (FCCP), rotenone, Antimycin A were purchased from Agilent (Santa Clara, CA, USA). Palmitic acid (C18:0) and all
98 other chemicals were obtained from Sigma-Aldrich (St Louis, MO, USA), except when specified.

99

100 **2.2. Cell culture treatments**

101 An established experimental model was used to culture and differentiate skeletal (C2C12) muscle cells [29].
102 Briefly, cells were cultured and sub-cultured in DMEM containing 4.5g/L glucose and 20 mM HEPES,
103 supplemented with 10% (v/v) FCS, 100 U/mL penicillin, and 100 μ g/mL penicillin-streptomycin for 3 days or until
104 90-100 % confluent. Upon confluency, these myoblasts were differentiated by switching to low serum DMEM
105 containing 2% HS to induce myotube formation. Then, C2C12 myotubules were seeded into cell bind 24-well
106 plates (25 000 cells/well), 96-well plates (5 000 cells/well) or 6-well plates (75 000 cells/well); and for seahorse,
107 96 well XF-96 microplate plates (12 000 cells/well) were used. Media was replaced every 48 h, on day 5 cells
108 were fully differentiated into myotubules, and then further experiments were performed.

109

110 **2.3. Induction of insulin resistance and treatment with aspalathin**

111 Upon confluence, insulin resistance was induced by culturing C2C12 myotubules in DMEM containing 2% BSA,
112 5.5 mM glucose and 0.75 mM palmitate for 16 h, as previously described [29]. On the other hand, experimental
113 control cells were cultured in DMEM without palmitate. After induction of insulin resistance, cells were serum
114 and glucose starved before treatment with aspalathin, which was prepared as previously described [21]. For
115 treatment, the cells were exposed for 1 h in either 1 μ M insulin (used as a positive control) or 10 μ M aspalathin
116 that was diluted in 2% BSA DMEM culture media with or without palmitate. Choice of dose and treatment time
117 for aspalathin was based on previously published research [21].

118

119 **2.4. Determination of cell viability and metabolic activity**

120 The PrestoBlue™ dye was used as a measure of cell viability, whilst the luminescent ATP kit was used to evaluate
121 metabolic activity. Briefly, after treatment 10 μ L PrestoBlue™ was added to each well and incubated for 40 min
122 at room temperature and absorbance (570 nm) was measured after 10 min using PHERAstar® plate reader (BMG
123 LABTECH, Germany). To measure the level of ATP within the cell, the luminescent ATP kit was used, as described
124 by the manufacturer. ATP luminescence was read using a BioTek FLx800 plate reader and Gen 5 software for
125 data acquisition (BioTek Instruments Inc., Winooski, VT, USA).

126

127 **2.5. Determination of glucose uptake**

128 Briefly, the glucose uptake test was performed using radiolabelled 2-Deoxy-[³H]-D-glucose, as previously
129 described [20, 21]. Briefly, after 16 h of incubation with palmitate and treatment with or without aspalathin for
130 1h, 0.5 μ Ci/mL 2-Deoxy-[³H]-D-glucose was added to each well and incubated at 37°C in 5% CO₂ and humidified
131 air for 15 min. Thereafter 2-Deoxy-[³H]-D-glucose as assessed by liquid scintillation using (2220 CA, Packard Tri-
132 Carb series, PerkinElmer, Downers Grove, IL, USA).

133

134 **2.6. mRNA expression analysis**

135 Total RNA was extracted from treated C2C12 myotubules using Qiazol buffer according to the manufacturer's
136 instructions, thereafter RNA concentration was determined using NanoDrop spectrophotometer (Thermo
137 Scientific, USA). To remove contaminating genomic DNA from RNA, samples were DNase treated using
138 QuantiTect Reverse Transcription Kit, and total RNA was reverse transcribed into cDNA according to the
139 manufacturer's recommendations. Differential gene expression was analysed by quantitative RT-PCR using
140 QuantStudio™ 6 (Applied Biosystems, CA, USA). Gene expression, for interleukin (*Il*)-6, tumor necrosis factor
141 alpha (*Tnf- α*), fatty acid transport protein 1 (*Fatp1*), carnitine palmitoyltransferase 1 (*Cpt1*), uncoupling protein
142 2 (*Ucp2*), NAD-dependent deacetylase sirtuin 1 (*Sirt1*), nuclear respiratory factor 1 (*Nrf1*) and transcription factor

143 A, mitochondrial (*Tfam*) was calculated as delta Ct using Actin beta (Act b) for normalization and relative to the
 144 untreated (experimental) control group normalized to a value of 100%, stated as “relative mRNA expression” in
 145 the y axis label. The list of gene expression probes used in this study as supplied in Table 1.

146 **Table 1. The list of mRNA probes used in the study.**

Probe	Role	Assay ID	147
Interleukin 6 (<i>Il6</i>)	Inflammation	Mm00446190_m1	148
Tumor necrosis factor alpha (<i>Tnf-α</i>),	Inflammation	Mm00443258_m1	149
fatty acid transport protein 1 (<i>Fatp1</i>),	Lipid metabolism	Mm00444340_m1	150
carnitine palmitoyltransferase 1 (<i>Cpt1</i>)	Lipid metabolism	Mm00487191_g1	151
Uncoupling Protein 2 (<i>Ucp2</i>)	Mitochondrial bioenergetics	Mm00627599_m1	152
Sirtuin (<i>Sirt1</i>)	Mitochondrial biogenesis	Mm01168521_m1	153
Nuclear Respiratory Factor 1 (<i>Nrf1</i>)	Mitochondrial biogenesis	Mm01135606_g1	154
transcription factor A, mitochondrial (<i>Tfam</i>)	Mitochondrial bioenergetics	Mm00447485_m1	155
Actin beta (<i>Act b</i>)	Housekeeping	Mm02619580_g1	155

156 2.7. Cellular bioenergetics

157 An established protocol was used to assess cellular bioenergetics [22, 30]. Briefly, before the measurements
 158 of cellular respiration, treated cells were removed from the CO₂ incubator and the media were changed to XF
 159 Assay Medium containing 8 mM glucose with or without palmitate, aspalathin or etomoxir (1 mM), then
 160 equilibrated for another hr at 37 °C without CO₂. Thereafter, the XF9-6 plate was transferred to a Seahorse XF96
 161 extracellular flux analyser (Agilent Technologies, Chicopee, MA 01022) and basal respiration/glycolysis values
 162 determined in three assay cycles (1 min mixing, 2 min waiting, 3 min measuring). Then, oligomycin (2 µg/ mL)
 163 was injected in port A, followed by FCCP (2.5 µM) injection in port B, rotenone and antimycin A (2.5 µM) port C
 164 and 2-Deoxy-[³H]-D-glucose (100 µM) in port D. Results were normalised to DNA using PicoGreen® dsDNA
 165 quantitation assay kit according to manufactures recommendations.

166

167 2.8. Western blot analysis

168 Western blot analysis was performed using a standardised protocol, as previously described [20, 29]. Briefly,
 169 protein was extracted using RIPA buffer, 40 µg for cells, was extracted using Tissue Lysis buffer (Qiagen)
 170 thereafter, heat denatured. Protein was separated on a 10 or 12% SDS-PAGE gel and transferred to a PVDF-P
 171 membrane. Successful transfer was determined using Ponceau stain, membrane was blocked with 5% (w/v) low-
 172 fat milk powder in Tris-buffered saline with Tween 20 (TBST) at room temperature for 2 h. Membranes were
 173 then labelled overnight at 4°C with the relevant primary antibody (PKC θ, p/PKC θ^(Ser 643/676), pAKT, tAKT, and IR)

174 and HRP conjugated secondary antibodies applied for 1½ h the following day. Proteins were detected and
175 quantified by chemiluminescence using a Chemidoc-XRS imager and Quantity One 1-D software (Biorad
176 Laboratories, Hercules, CA, USA), respectively. Here, β-actin was used as the reference control.

177

178 **2.9. Statistical analysis**

179 All results are expressed as ± standard error of the mean (SEM) of three independent biological experiments.
180 The significant difference between groups was determined using one-way of variance (ANOVA) followed by
181 Tukey's post hoc test using GraphPad Prism version 8.0.1 (GraphPad Software Inc., San Diego, CA, USA). Results
182 were considered significant at $p \leq 0.05$. For PCR results, comparisons between groups were performed using
183 one-way multivariate ANOVA, followed by unpaired Student *t*-test, and a *p*-value of ≤ 0.05 was deemed as
184 statistically significant.

185

186 **3. Results**

187 **3.1. Aspalathin restored cell viability and ATP production in palmitate-induced insulin-resistant C2C12** 188 **myotubules**

189 The effects of palmitate and aspalathin on cell viability and metabolic activity were investigated in differentiated
190 C2C12 myotubules. The results showed that insulin has an ability to improve cell viability and ATP production in
191 normal cells (not exposed to palmitate) ($p < 0.05$ and $p < 0.001$, respectively) (Figure 1A, B). Interestingly, 0.75
192 mM palmitate significantly reduced cell viability ($p < 0.01$) and ATP production ($p < 0.001$) when compared to
193 experimental (normal) controls (Figure 1A, B). The addition of aspalathin, either as a monotherapy or in
194 combination with insulin, significantly improved cell viability ($p < 0.001$ and $p < 0.01$, respectively) and ATP
195 production ($p < 0.001$) in cells exposed to palmitate (Figure 1A, B). However, insulin, as a positive control did not
196 have a significant effect in improving cell viability and ATP production in comparison in cells exposed to palmitate
197 (Figure 1A, B).

198

199 **Figure 1. Effect of aspalathin on cell viability (A) and energy production (ATP) (B) in insulin resistant skeletal muscle (C2C12)**
200 **cells.** Briefly, C2C12 myotubules were treated with or without 0.75 mM palmitate for 16 h, thereafter cultured with aspalathin
201 (10 μM) for 1 h, while insulin (1 μM) was added in the last 15 min as a positive control. As an endpoint measurement, cell
202 viability was assessed by prestoBlue dye and energy production (ATP) by luminescent ATP kit. Results are expressed as the
203 mean of three independent experiments relative to the control at 100% ± SEM. * $p < 0.05$, ** $p < 0.01$, *** $p < 0.001$ versus
204 experimental control. ## $p < 0.01$, ### $p < 0.001$ versus palmitate control.

205

206 **3.2. Aspalathin improved glucose uptake and the expression levels of proteins involved insulin signaling in**
207 **palmitate-induced insulin resistant C2C12 myotubules**

208 Determining the levels of cellular glucose uptake, including the modulation of protein markers involved in insulin
209 signaling like AKT/IR remains essential to evaluate the capability of treatment compounds to ameliorate insulin
210 resistance. Insulin as comparative control, significantly improved glucose uptake ($p < 0.001$) and the
211 phosphorylation of AKT in the normal cells ($p < 0.001$) (Figure 2A, B and C). However, exposure of C2C12
212 myotubules to 0.75 mM palmitate significantly suppressed glucose uptake ($p < 0.01$), including protein
213 expression levels of IR (not statistically significant) and p/AKT ($p < 0.001$) when compared to an experimental
214 control (Figure 2A, B, and C). Nonetheless, treatment with aspalathin, as monotherapy or in combination with
215 insulin, improved glucose uptake ($p < 0.001$), IR protein expression ($p < 0.01$ and $p < 0.001$), and the
216 phosphorylation of AKT ($p < 0.001$) (Figure 2A, B and C). Notably, insulin as a comparative control, showed similar
217 results to aspalathin relevant to glucose uptake ($p < 0.01$) and p/AKT ($p < 0.001$) in palmitate exposed cells (Figure
218 2).

219

220 **Figure 2. Effect of aspalathin on glucose uptake (A), and protein expression levels of insulin receptor (IR; B), and**
221 **phosphorylated protein kinase B (p/AKT; C) in insulin resistant skeletal muscle (C2C12) cells.** Briefly, C2C12 myotubules
222 were treated with or without 0.75 mM palmitate for 16 h, thereafter cultured with aspalathin (10 μ M) for 1 h, while insulin
223 (1 μ M) was added in the last 15 min as a positive control. Treated cells were lysed and subjected to Western blot analysis.
224 Results are expressed as the mean of three independent experiments relative to control set at 100% \pm SEM ** $p < 0.01$, *** $p <$
225 0.001 versus experimental control: ## $p < 0.01$, ### $p < 0.001$ versus palmitate control.

226

227 **3.3. Aspalathin improved gene expression levels of some molecular markers of fatty acid transport and**
228 **inflammation in palmitate-induced insulin resistant C2C12 myotubules**

229 Briefly, aberrant cellular fatty acid transportation, which may lead to the downstream detrimental effects of
230 inflammation, remains an important aspect to determine, as it is also linked with the exacerbation of insulin
231 resistance. Accordingly, exposure of differentiated C2C12 myotubules to 0.75 mM palmitate resulted in
232 markedly increased mRNA expression levels of fatty acid transporters like *Fatp1* ($p < 0.001$) and *Cpt1* ($p < 0.001$),
233 including prominent markers of inflammation such as *Il-6* ($p < 0.001$), *Tnf- α* ($p < 0.001$), and PKC- θ ($p < 0.001$) in
234 comparison to the experimental control (Figure 3A-E). Treatment with aspalathin, either as a monotherapy or
235 in combination with insulin, showed comparative results in significantly reducing these fatty acid transport and
236 inflammation makers. Notably, insulin as a positive control, did not significantly affect the mRNA expression
237 levels of *Fatp1* and *Cpt1*, or pro-inflammatory markers (*Il-6*, *Tnf- α* and PKC- θ) in comparison to palmitate only
238 exposed cells (Figure 3).

239

240 **Figure 3. Effect of aspalathin on the regulation of mRNA expression levels of genes involved in beta-oxidation like fatty**
241 **acid transport protein 1 (Fatp1; A) carnitine palmitoyltransferase 1 (Cpt1; B), and genes involved in inflammation such as**
242 **interleukin-6 (Il6; C) and tumor necrosis factor alpha (TNF- α ; D), as well as protein expression of protein kinase C theta**
243 **(PKC- θ ; E) in insulin resistant skeletal muscle (C2C12) cells. Briefly, C2C12 myotubules were treated with or without 0.75 mM**
244 **palmitate for 16 h, thereafter cultured with aspalathin (10 μ M) for 1 h, while insulin (1 μ M) was added in the last 15 min as**
245 **a positive control. Treated cells were lysed and quantified by RT-PCR and protein analysis. Results are expressed as the mean**
246 **of three independent experiments relative to control set at 100% \pm SEM. *** p < 0.001 versus experimental control: ## p < 0.01,**
247 **### p < 0.001 versus palmitate control.**

248

249 **3.4. Aspalathin improved cellular bioenergetics in palmitate-induced insulin resistant C2C12 myotubules**

250 To characterize the effect of aspalathin on the process of mitochondrial bioenergetics, we measured the OCR
251 (Figure 5A) and ECAR (Figure 5B) in palmitate-induced insulin resistant C2C12 myotubules using Agilent Seahorse
252 XF Technology. After induction of insulin resistance with palmitate for 16 h, muscle cells displayed significantly
253 suppressed basal OCR (p < 0.01), ATP production (p < 0.01), maximal respiration (p < 0.001), and spare
254 respiratory capacity (p < 0.05) (Figure 4C-F). Treatment with aspalathin showed comparative results to its
255 combination with insulin in improving all markers of mitochondrial bioenergetics (Figure 4C-F). The use of
256 insulin, as a comparative control, failed to show any effect (except for increasing maximal respiration, p < 0.001)
257 in improving mitochondrial bioenergetics using the current experimental model of C2C12 myotubules exposed
258 to elevated concentrations of palmitate.

259

260 **Figure 4. Effect of aspalathin on the regulation of mitochondrial bioenergetics, including basal oxygen consumption rate**
261 **(OCR; A) and extracellular acidification rates (ECAR; B) of all treatments, before independent analysis of basal OCR (C),**
262 **adenosine triphosphate (ATP) production (D), maximal respiration (E), and spare respiratory capacity (F) in insulin resistant**
263 **skeletal muscle (C2C12) cells. Briefly, C2C12 myotubules were treated with or without 0.75 mM palmitate for 16 h, thereafter**
264 **cultured with aspalathin (10 μ M) for 1 h, while insulin (1 μ M) was added in the last 15 min as a positive control. The OCR and**
265 **ECAR were determined using Seahorse XF-96 Metabolic Flux Analyzer. Groups (A, B, C, D, E and F) show data of changes in**
266 **OCR, ECAR, in response to the sequential administration (arrows) of oligomycin (2 μ g/ mL) port A, Carbonyl cyanide-*p*-**
267 **trifluoromethoxyphenylhydrazone (FCCP) (2.5 μ M) port B, antimycin and Rotenone (2.5 μ M) port C. Results are expressed as**
268 **mean \pm SEM of 3 independent experiments. * p \leq 0.05, ** p < 0.001 *** p < 0.001 versus experimental control; # p < 0.05, ## p <**
269 **0.05### p < 0.001 versus palmitate control.**

270

271 **3.5. Aspalathin improved the expression levels of genes involved in mitochondrial energetics in palmitate-**

272 **induced insulin resistant C2C12 myotubules**

273 We further investigated the effect of aspalathin on the expression levels of genes involved in mitochondrial
274 energetics in palmitate induced C2C12 myotubules. Here, exposure of differentiated C2C12 myotubules to 0.75

275 mM palmitate significantly reduced the mRNA expression levels of *Ucp2* ($p < 0.001$), *Sirt1* ($p < 0.001$), *Nrf1* ($p <$
276 0.001), and *Tfam* ($p < 0.001$) (Figure 5A-D). Interestingly, also consistent with Seahorse data (Figure 4), treatment
277 with aspalathin, either as a monotherapy or in combination with insulin, significantly improved the expression
278 levels of all analyzed genes ($p < 0.001$) (Figure 5A-D). The use of insulin, as a comparative control, showed some
279 effect in enhancing the expression *Ucp2* ($p < 0.001$), *Sirt1* ($p < 0.001$), *Nrf1* ($p < 0.001$), and *Tfam* ($p < 0.001$) in
280 comparison to palmitate control (Figure 5).

281

282 **Figure 5. Effect of aspalathin on the regulation of mRNA expression levels of genes involved mitochondrial function,**
283 **including uncoupling protein 2 (*Ucp2*; A), silent mating type information regulation 2 homolog (*Sirt1*; B), nuclear**
284 **respiratory factor 1 (*Nrf1*; C) and transcription factor A, mitochondrial (*Tfam*; D) in insulin resistant skeletal muscle (C2C12)**
285 **cells. Briefly, C2C12 myotubules were treated with or without 0.75 mM palmitate for 16 h, thereafter cultured with aspalathin**
286 **(10 μ M) for 1 h, while insulin (1 μ M) was added in the last 15 min as a positive control. Treated cells were lysed and quantified**
287 **by RT-PCR analysis. Results are expressed as the mean of three independent experiments relative to control set at 100% \pm**
288 **SEM. *** $p < 0.001$ versus experimental control; ### $p < 0.001$ versus palmitate control.**

289

290 4. Discussion

291 Pathological features, insulin resistance and mitochondrial dysfunction, are known hallmarks of T2DM, and are
292 widely studied through the application of diverse preclinical models that mimic human disease [31-33]. Research
293 from our group has explored an in vitro model of exposing cultured cells to elevated concentrations of palmitate
294 as a feasible strategy to study pathological mechanisms of T2DM, including the development of insulin resistance
295 and mitochondrial dysfunction [21, 29, 34, 35]. In fact, there has been a growing interest in understanding the
296 cause-effect relationship between insulin resistance and mitochondrial dysfunction during the pathogenesis of
297 T2DM, especially within the skeletal muscle [31-33]. As such, beyond inducing alterations in substrate
298 metabolism which may be characterized by suppressed glucose metabolism, exposing cultured cells to elevated
299 concentrations of palmitate (0.75 mM) for 16 h has been shown to significantly hinder the process of
300 mitochondrial respiration, including reducing the expression of major genes involved insulin signaling and
301 mitochondrial function [22, 36]. Other studies have reported that oxidative stress, which is often exacerbated
302 by mitochondrial dysfunction, might also accelerate cellular apoptosis, a consequence that has been explored
303 in experimental models of metabolic disease [37, 38]. Indeed, previous reviews have critically discussed the
304 pathological role of apoptosis in the development of T2DM, especially its implication in the destruction of
305 pancreatic β - islet cells [39, 40]. Further, highlighting the importance of understanding the pathological features
306 of T2DM, specifically mitochondrial dysfunction in order to protect against destructive processes involving
307 apoptosis or accelerated cell death.

308 Notably, palmitate exposure, as an experimental model to mimic the toxic effects of lipid overload, has been
309 increasingly studied [41]. In fact, the current study showed that exposing skeletal muscle (C2C12) myotubules
310 to elevated concentrations of palmitate could effectively reduce glucose uptake and cell viability, and this was
311 consistent with suppressing mitochondrial respiration, including genes involved in this process, such as *Ucp2*,
312 *Sirt1*, *Nrf1*, and *Tfam*. Interestingly, also to further characterize the classical features T2DM, the current study
313 also showed that exposing C2C12 myotubules to elevated concentrations of palmitate resulted in enhanced
314 levels of molecular makers indicating an abnormal inflammatory response, such as the mRNA levels of *Il-6*, *Tnf-*
315 α , and phosphorylation of PKC- θ . This certainly affirms the relevance of using this in vitro model, of exposing
316 C2C12 cells to elevated concentrations of palmitate, to assess the therapeutic effects of aspalathin against
317 T2DM-related complications, including insulin resistance, mitochondrial dysfunction and an abnormal
318 inflammatory response.

319 Intriguingly, research has progressively explored the use of plant-derived sources for their ameliorative effects
320 against skeletal muscle insulin resistance, through the application of in vitro techniques. For example, the
321 blueberry leaf extract was shown to attenuate TNF- α -induced insulin resistance by promoting glucose uptake
322 and improving insulin signaling via upregulating AKT phosphorylation in cultured skeletal (C2C12) myotubules
323 [42]. Alternatively, the well-known phytochemicals like quercetin, rutin and gallic acid, found in rooibos and
324 other food sources, have been shown to hinder skeletal muscle atrophy and block cell apoptosis, in part by
325 effectively scavenging for free radical species and improving mitochondrial function in cultured in C2C12
326 myotubules [43, 44]. Here, the major results showed that aspalathin treatment could alleviate palmitate-
327 induced skeletal muscle insulin resistance by enhancing glucose uptake and mitochondrial respiration, blocking
328 FFA-transport, as well as improving insulin signaling as partly demonstrated through increased phosphorylation
329 of AKT in cultured C2C12 myotubules (Figure 6). Interestingly, such findings are consistent with findings from
330 other cellular models, mimicking complications of T2DM, reporting on the bioactive properties from rooibos,
331 including aspalathin [22, 35, 36]. Furthermore, it has been reported that inflammation also plays a major role in
332 the development of T2DM [45]. For example, macrophages and other immunocompetent cells can modulate an
333 immune response and subsequently an inflammatory state through their secretion of cytokines such as TNF- α
334 and IL-6, further taking part in different immune responses and protection against pathogens and diseases [46,
335 47]. However, excessive immune activation, or exacerbated secretion of these pro-inflammatory cytokines has
336 been implicated in the deterioration of metabolic complications linked with T2DM [46, 48]. Similarly, there was
337 increased mRNA expression of *TNF- α* and *IL-6* upon the exposure of cells to palmitate in the current study. Such
338 findings promote an important aspect entailing on the anti-inflammatory properties of this dihydrochalcone, as
339 it effectively blocked PKC- θ phosphorylation in addition to reducing the mRNA levels of *Il-6* and *Tnf- α* in these
340 palmitate-exposed skeletal muscle cells. In fact, this is validating the hypothesis that beyond its free radical
341 scavenging properties [49], aspalathin presents with enhanced ameliorative effects against inflammation [50].

342

343 Figure 6: An overview of therapeutic mechanisms by which aspalathin ameliorates palmitate-induced insulin resistance in
344 skeletal muscle (C2C12) myotubules. Briefly, the major results in this study showed that aspalathin treatment could alleviate
345 palmitate-induced skeletal muscle insulin resistance by enhancing glucose uptake and mitochondrial respiration blocking
346 free fatty acid (FFA)-transport, as well as improving insulin signaling as partly demonstrated through increased expression
347 insulin receptor (IR)/phosphorylation of protein kinase B (AKT) in cultured C2C12 myotubules. This bioactive compound could
348 effectively attenuate inflammation by reducing the expression of markers such as interleukin-6 (*IL-6*), tumor necrosis factor-
349 alpha (*TNF-α*), and protein kinase C-theta (PKC-θ). Moreover, markers of mitochondrial function included, included
350 uncoupling protein 2 (*Ucp2*), NAD-dependent deacetylase sirtuin 1 (*Sirt1*), nuclear respiratory factor 1 (*Nrf1*) and
351 transcription factor A, mitochondrial (*Tfam*).

352

353 5. Conclusions

354 Through the use of in vitro model of skeletal muscle insulin resistance, the current results support the notion
355 that aspalathin presents with an enhanced therapeutic capacity to ameliorate diverse complications of
356 metabolic syndrome, as previously reviewed [19]. Although such information remains relevant and could
357 enhance the therapeutic development of aspalathin as a potential nutraceutical, the current study is not without
358 limitations. Firstly, it remains essential to confirm these results using an established in vivo model of T2DM.
359 Importantly, the in vivo model of T2DM could be used for a complete analysis of molecular mechanisms, linking
360 both insulin resistance and mitochondrial dysfunction to better understand the therapeutic benefits of
361 aspalathin and its potential synergetic effect with insulin (especially making use of in vivo models of T2DM).
362 Notably, although insulin can be used as an effective comparative control [36, 51], other reference drugs,
363 especially those specific for T2DM like metformin will add value to the understanding of therapeutic benefits of
364 aspalathin in future studies. Lastly, future studies should also look the therapeutic effects of aspalathin against
365 oxidative stress-related cell death within the skeletal muscle, including the implications of inflammation during
366 the development of T2DM.

367

368 Abbreviations

369 **AKT**, protein kinase B; **Cpt1**, carnitine palmitoyltransferase 1; **ECAR**, extracellular acidification rate; **Fatp1**, fatty
370 acid transport protein 1; **FFA**, free fatty acids; **IL-6**, interleukin-6; **IR**, insulin receptor; **Nrf1**, nuclear respiratory
371 factor 1; **OCR**, mitochondrial oxygen consumption rate; **PI3K**, phosphoinositide 3-kinase; **PKC-θ**, protein kinase
372 C-theta; **Sirt1**, NAD-dependent deacetylase sirtuin 1; **T2DM**, Type 2 diabetes mellitus; **Tfam**, transcription factor
373 A; **TNF-α**, tumor necrosis factor-alpha; **Ucp2**, uncoupling protein 2

374

375 Funding statement

376 This work was funded by the National Research Foundation (NRF) of South Africa Thuthuka Programme grant
377 128296 and NRF support for rated scientist 113674 to S.E. Mazibuko-Mbeje. Baseline funding from the
378 Biomedical Research and Innovation Platform of the South African Medical Research Council (SAMRC) and
379 Northwest University is also acknowledged. Grant holders acknowledge that opinions, findings and conclusions
380 or recommendations expressed in any publication generated by the NRF or SAMRC supported research are those
381 of the authors, and that the NRF or SAMRC accepts no liability whatsoever in this regard.

382

383 **Acknowledgements**

384 The authors, S.X.H. Mthembu and K. Ziqubu, are funded by the SAMRC through its Division of Research Capacity
385 Development under the internship scholarship program from funding received from the South African National
386 Treasury. Grant holders acknowledge that opinions, findings and conclusions or recommendations expressed in
387 any publication generated by the SAMRC supported research are those of the authors, and that the SAMRC
388 accepts no liability whatsoever in this regard.

389

390 **Declaration of competing interest**

391 The authors declare no conflict of interest.

392

393 **Authors' contributions**

394 S.E. Mazibuko-Mbeje, C.J.F. Muller, and P.V. Dlodla - concept and original draft; S.E. Mazibuko-Mbeje, S.X.H.
395 Mthembu, K. Ziqubu, N. Muvhulawa, and R.V. Modibedi - performed the experiments and data analysis; S.E.
396 Mazibuko-Mbeje- funding and resources; S.E. Mazibuko-Mbeje, C.J.F. Muller, S.X.H. Mthembu, K. Ziqubu, N.
397 Muvhulawa, R.V. Modibedi, L. Tiano, P.V. Dlodla - manuscript writing and approval of the final draft.

398

399 **Data availability statement**

400 Data related to search strategy, study selection and extraction items will be made available upon request after
401 the manuscript is published.

402

403

404 **References**

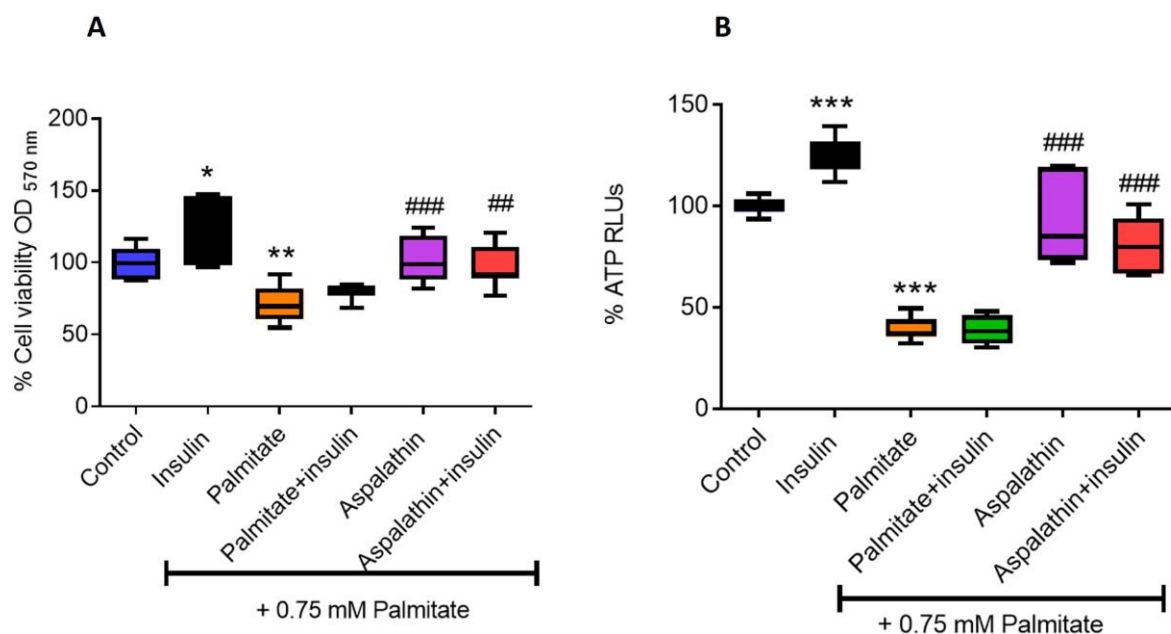
- 405 1. International Diabetes Federation, IDF Diabetes Atlas 2021. Available at: <https://diabetesatlas.org/>.
406 Accessed 02 January 2022.
- 407 2. World Health Organization (WHO), The top ten leading causes of death. Available at:
408 <https://www.who.int/news-room/fact-sheets/detail/the-top-10-causes-of-death>. Accessed 03 January
409 2022.
- 410 3. Grundy SM. Metabolic syndrome update. *Trends Cardiovasc Med* 2016;26(4):364-73.
- 411 4. DeFronzo RA, and Tripathy D. Skeletal muscle insulin resistance is the primary defect in type 2 diabetes.
412 *Diabetes Care* 2009;32 Suppl 2(Suppl 2):S157-63.
- 413 5. Hargreaves M, and Spriet LL. Skeletal muscle energy metabolism during exercise. *Nat Metab*
414 2020;2(9):817-828.
- 415 6. Wojtaszewski JF, and Richter EA. Glucose utilization during exercise: influence of endurance training.
416 *Acta Physiol Scand* 1998;162(3):351-8.
- 417 7. Evans PL, McMillin SL, Weyrauch LA, and Witczak CA. Regulation of skeletal muscle glucose transport
418 and glucose metabolism by exercise training. *Nutrients* 2019;11(10):2432.
- 419 8. Chang L, Chiang SH, Saltiel AR. Insulin signaling and the regulation of glucose transport. *Molecular*
420 *medicine* 2004;10(7):65-71.
- 421 9. Rena G, Hardie DG, Pearson ER. The mechanisms of action of metformin. *Diabetologia* 2017;
422 60(9):1577-85.
- 423 10. Foretz M, Guigas B, Bertrand L, Pollak M, Viollet B. Metformin: from mechanisms of action to therapies.
424 *Cell metabolism* 2014;20(6):953-66.
- 425 11. Petersen MC, Shulman GI. Mechanisms of insulin action and insulin resistance. *Physiological reviews*
426 2018;98(4):2133-223..
- 427 12. Li J, Bai L, Wei F, Zhao J, Wang D, Xiao Y, Yan W, Wei J. Therapeutic mechanisms of herbal medicines
428 against insulin resistance: a review. *Frontiers in Pharmacology* 2019 ;10:661.
- 429 13. Cui X, Qian DW, Jiang S, Shang EX, Zhu ZH, Duan JA. *Scutellariae radix* and *coptidis rhizoma* improve
430 glucose and lipid metabolism in T2DM rats via regulation of the metabolic profiling and MAPK/PI3K/Akt
431 signaling pathway. *International journal of molecular sciences* 2018;19(11):3634.
- 432 14. Kuai M, Li Y, Sun X, Ma Z, Lin C, Jing Y, Lu Y, Chen Q, Wu X, Kong X, Bian H. A novel formula Sang-Tong-
433 Jian improves glycometabolism and ameliorates insulin resistance by activating PI3K/AKT pathway in
434 type 2 diabetic KKAY mice. *Biomedicine & Pharmacotherapy* 2016;84:1585-94.

- 435 15. Joubert ED, de Beer D. Rooibos (*Aspalathus linearis*) beyond the farm gate: From herbal tea to potential
436 phytopharmaceutical. *South African Journal of Botany* 2011;77(4):869-86.
- 437 16. Muller CJ, Malherbe CJ, Chellan N, Yagasaki K, Miura Y, Joubert E. Potential of rooibos, its major C-
438 glucosyl flavonoids, and Z-2-(β -D-glucopyranosyloxy)-3-phenylpropenoic acid in prevention of
439 metabolic syndrome. *Critical Reviews in Food Science and Nutrition* 2018;58(2):227-46.
- 440 17. Dlodla PV, Joubert E, Muller CJ, Louw J, Johnson R. Hyperglycemia-induced oxidative stress and heart
441 disease-cardioprotective effects of rooibos flavonoids and phenylpyruvic acid-2-O- β -D-glucoside.
442 *Nutrition & metabolism* 2017;14(1):1-8.
- 443 18. Abdul NS, Marnewick JL. Rooibos, a supportive role to play during the COVID-19 pandemic?. *Journal of*
444 *Functional Foods* 2021;86:104684.
- 445 19. Johnson R, de Beer D, Dlodla PV, Ferreira D, Muller CJ, Joubert E. Aspalathin from rooibos (*Aspalathus*
446 *linearis*): a bioactive C-glucosyl dihydrochalcone with potential to target the metabolic syndrome.
447 *Planta medica* 2018;84(09/10):568-83.
- 448 20. Johnson R, Dlodla P, Joubert E, February F, Mazibuko S, Ghoor S, Muller C, Louw J. Aspalathin, a
449 dihydrochalcone C-glucoside, protects H9c2 cardiomyocytes against high glucose induced shifts in
450 substrate preference and apoptosis. *Molecular nutrition & food research* 2016;60(4):922-34.
- 451 21. Mazibuko SE, Joubert E, Johnson R, Louw J, Opoku AR, Muller CJ. Aspalathin improves glucose and lipid
452 metabolism in 3T3-L1 adipocytes exposed to palmitate. *Molecular nutrition & food research*
453 2015;59(11):2199-208.
- 454 22. Mazibuko-Mbeje SE, Dlodla PV, Johnson R, Joubert E, Louw J, Ziqubu K, Tiano L, Silvestri S, Orlando P,
455 Opoku AR, Muller CJ. Aspalathin, a natural product with the potential to reverse hepatic insulin
456 resistance by improving energy metabolism and mitochondrial respiration. *PloS one* 2019
457 ;14(5):e0216172.
- 458 23. Kawano A, Nakamura H, Hata SI, Minakawa M, Miura Y, Yagasaki K. Hypoglycemic effect of aspalathin,
459 a rooibos tea component from *Aspalathus linearis*, in type 2 diabetic model db/db mice. *Phytomedicine*
460 2009;16(5):437-43.
- 461 24. Ku SK, Kwak S, Kim Y, Bae JS. Aspalathin and nothofagin from rooibos (*Aspalathus linearis*) inhibits high
462 glucose-induced inflammation in vitro and in vivo. *Inflammation* 2015;38(1):445-55.
- 463 25. Smit SE, Johnson R, Van Vuuren MA, Huisamen B. Myocardial glucose clearance by aspalathin treatment
464 in young, mature, and obese insulin-resistant rats. *Planta Medica* 2018;84(02):75-82.

- 465 26. Muller CJ, Joubert E, De Beer D, Sanderson M, Malherbe CJ, Fey SJ, Louw J. Acute assessment of an
466 aspalathin-enriched green rooibos (*Aspalathus linearis*) extract with hypoglycemic potential.
467 *Phytomedicine* 2012;20(1):32-9.
- 468 27. Mazibuko-Mbeje SE, Dlodla PV, Roux C, Johnson R, Ghoor S, Joubert E, Louw J, Opoku AR, Muller CJ.
469 Aspalathin-enriched green rooibos extract reduces hepatic insulin resistance by modulating PI3K/AKT
470 and AMPK pathways. *International journal of molecular sciences* 2019;20(3):633.
- 471 28. Johnson R, Shabalala S, Louw J, Kappo AP, Muller CJ. Aspalathin reverts doxorubicin-induced
472 cardiotoxicity through increased autophagy and decreased expression of p53/mTOR/p62 signaling.
473 *Molecules* 2017;22(10):1589.
- 474 29. Mazibuko SE, Muller CJ, Joubert E, De Beer D, Johnson R, Opoku AR, Louw J. Amelioration of palmitate-
475 induced insulin resistance in C2C12 muscle cells by rooibos (*Aspalathus linearis*). *Phytomedicine*
476 2013;20(10):813-9.
- 477 30. Mazibuko-Mbeje SE, Mthembu SX, Dlodla PV, Madoroba E, Chellan N, Kappo AP, Muller CJ. Antimycin
478 A-induced mitochondrial dysfunction is consistent with impaired insulin signaling in cultured skeletal
479 muscle cells. *Toxicology in Vitro* 2021;76:105224.
- 480 31. Das M, Saucedo C, Webster NJ. Mitochondrial dysfunction in obesity and reproduction. *Endocrinology*
481 2021;162(1):bqaa158.
- 482 32. Mthembu SX, Dlodla PV, Nyambuya TM, Kappo AP, Madoroba E, Ziqubu K, Nyawo TA, Nkambule BB,
483 Silvestri S, Muller CJ, Mazibuko-Mbeje SE. Experimental models of lipid overload and their relevance in
484 understanding skeletal muscle insulin resistance and pathological changes in mitochondrial oxidative
485 capacity. *Biochimie* 2021 .
- 486 33. Sergi D, Naumovski N, Heilbronn LK, Abeywardena M, O'Callaghan N, Lionetti L, Luscombe-Marsh N.
487 Mitochondrial (Dys) function and insulin resistance: from pathophysiological molecular mechanisms to
488 the impact of diet. *Frontiers in physiology* 2019;10:532.
- 489 34. Dlodla PV, Silvestri S, Orlando P, Mazibuko-Mbeje SE, Johnson R, Marcheggiani F, Cirilli I, Muller CJ,
490 Louw J, Chellan N, Obonye N. Palmitate-induced toxicity is associated with impaired mitochondrial
491 respiration and accelerated oxidative stress in cultured cardiomyocytes: The critical role of coenzyme
492 Q9/10. *Toxicology in Vitro* 2020;68:104948.
- 493 35. Mazibuko-Mbeje SE, Ziqubu K, Dlodla PV, Tiano L, Silvestri S, Orlando P, Nyawo TA, Louw J, Kappo AP,
494 Muller CJ. Isoorientin ameliorates lipid accumulation by regulating fat browning in palmitate-exposed
495 3T3-L1 adipocytes. *Metabolism Open* 2020;6:100037.

- 496 36. Mazibuko-Mbeje SE, Mthembu SX, Tshiitamune A, Muvhulawa N, Mthiyane FT, Ziqubu K, Muller CJ,
497 Dlodla PV. Orientin Improves Substrate Utilization and the Expression of Major Genes Involved in Insulin
498 Signaling and Energy Regulation in Cultured Insulin-Resistant Liver Cells. *Molecules* 2021;26(20):6154.
- 499 37. M Victor V, Rocha M, Herance R, Hernandez-Mijares A. Oxidative stress and mitochondrial dysfunction
500 in type 2 diabetes. *Current pharmaceutical design* 2011;17(36):3947-58.
- 501 38. Dlodla PV, Jack B, Viraragavan A, Pheiffer C, Johnson R, Louw J, Muller CJ. A dose-dependent effect of
502 dimethyl sulfoxide on lipid content, cell viability and oxidative stress in 3T3-L1 adipocytes. *Toxicology*
503 *reports* 2018;5:1014-20.
- 504 39. Tomita T. Apoptosis of pancreatic β -cells in Type 1 diabetes. *Bosnian journal of basic medical sciences*
505 2017;17(3):183.
- 506 40. Kilanowska A, Ziłkowska A. Apoptosis in Type 2 Diabetes: Can It Be Prevented? Hippo Pathway
507 Prospects. *International Journal of Molecular Sciences* 2022;23(2):636.
- 508 41. Gunaratnam K, Vidal C, Boadle R, Thekkedam C, Duque G. Mechanisms of palmitate-induced cell death
509 in human osteoblasts. *Biology open* 2013;2(12):1382-9.
- 510 42. Yamasaki M, Hamada K, Fujii K, Nishiyama K, Yamasaki Y, Tari H, Araki K, Arakawa T. Vaccinium ashei
511 leaves extract alleviates insulin resistance via AMPK independent pathway in C2C12 myotube model.
512 *Biochemistry and biophysics reports* 2018;14:182-7.
- 513 43. Chen C, Yang JS, Lu CC, Chiu YJ, Chen HC, Chung MI, Wu YT, Chen FA. Effect of Quercetin on
514 Dexamethasone-Induced C2C12 Skeletal Muscle Cell Injury. *Molecules* 2020;25(14):3267.
- 515 44. Chang WT, Huang SC, Cheng HL, Chen SC, Hsu CL. Rutin and gallic acid regulates mitochondrial functions
516 via the SIRT1 pathway in C2C12 myotubes. *Antioxidants* 2021;10(2):286.
- 517 45. Tsalamandris S, Antonopoulos AS, Oikonomou E, Papamikroulis GA, Vogiatzi G, Papaioannou S,
518 Deftereos S, Tousoulis D. The role of inflammation in diabetes: current concepts and future
519 perspectives. *European cardiology review* 2019;14(1):50.
- 520 46. Bu L, Cao X, Zhang Z, Wu H, Guo R, Ma M. Decreased secretion of tumor necrosis factor- α attenuates
521 macrophages-induced insulin resistance in skeletal muscle. *Life Sciences* 2020;244:117304.
- 522 47. Juhas U, Ryba-Stanisławowska M, Szargiej P, Myśliwska J. Different pathways of macrophage activation
523 and polarization. *Advances in Hygiene & Experimental Medicine/Postepy Higieny i Medycyny*
524 *Doswiadczalnej* 2015;69.
- 525 48. Mahlangu T, Dlodla PV, Nyambuya TM, Mxinwa V, Mazibuko-Mbeje SE, Cirilli I, Marcheggiani F, Tiano
526 L, Louw J, Nkambule BB. A systematic review on the functional role of Th1/Th2 cytokines in type 2
527 diabetes and related metabolic complications. *Cytokine* 2020;126:154892.

- 528 49. Snijman PW, Joubert E, Ferreira D, Li XC, Ding Y, Green IR, Gelderblom WC. Antioxidant activity of the
 529 dihydrochalcones aspalathin and nothofagin and their corresponding flavones in relation to other
 530 rooibos (*Aspalathus linearis*) flavonoids, epigallocatechin gallate, and Trolox. *Journal of agricultural and*
 531 *food chemistry* 2009;57(15):6678-84.
- 532 50. Lee W, Bae JS. Anti-inflammatory effects of aspalathin and nothofagin from rooibos (*Aspalathus*
 533 *linearis*) in vitro and in vivo. *Inflammation* 2015;38(4):1502-16.
- 534 51. Sanvee GM, Bouitbir J, Krähenbühl S. Insulin prevents and reverts simvastatin-induced toxicity in C2C12
 535 skeletal muscle cells. *Scientific reports* 2019;9(1):1-0.
- 536
- 537



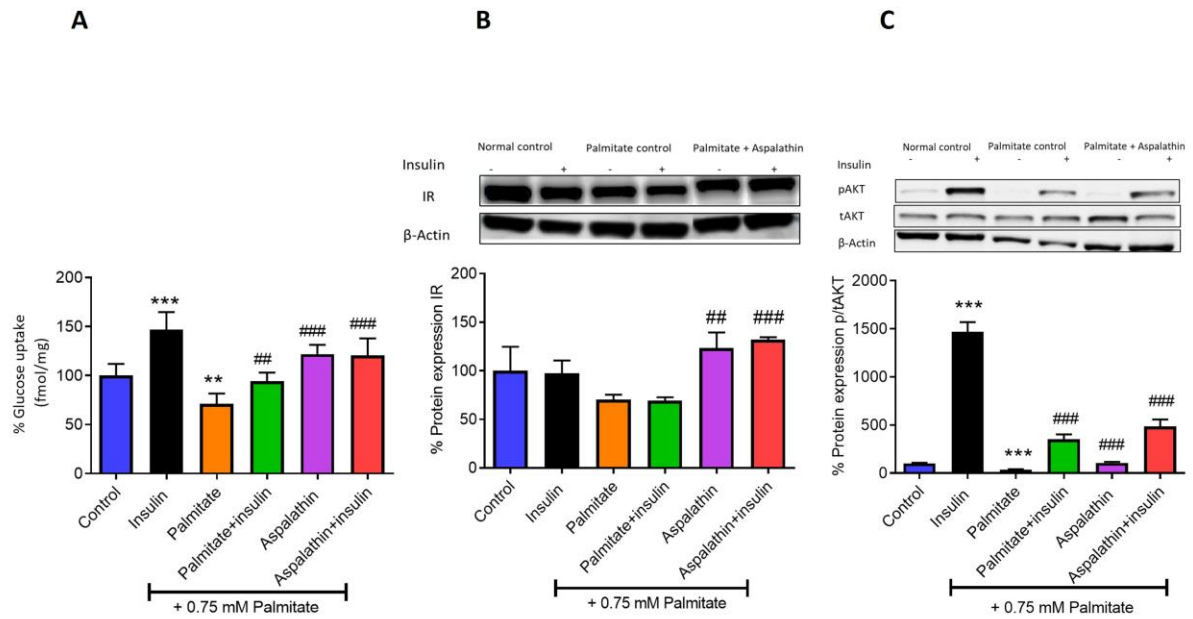
538

539 **Figure 1. Effect of aspalathin on cell viability (A) and energy production (ATP) (B) in insulin resistant skeletal muscle (C2C12)**
 540 **cells.** Briefly, C2C12 myotubules were treated with or without 0.75 mM palmitate for 16 h, thereafter cultured with aspalathin
 541 (10 μ M) for 1 h, while insulin (1 μ M) was added in the last 15 min as a positive control. As an endpoint measurement, cell
 542 viability was assessed by prestoBlue dye and energy production (ATP) by luminescent ATP kit. Results are expressed as the
 543 mean of three independent experiments relative to the control at 100% \pm SEM. * p < 0.05, ** p < 0.01, *** p < 0.001 versus
 544 experimental control. ## p < 0.01, ### p < 0.001 versus palmitate control.

545

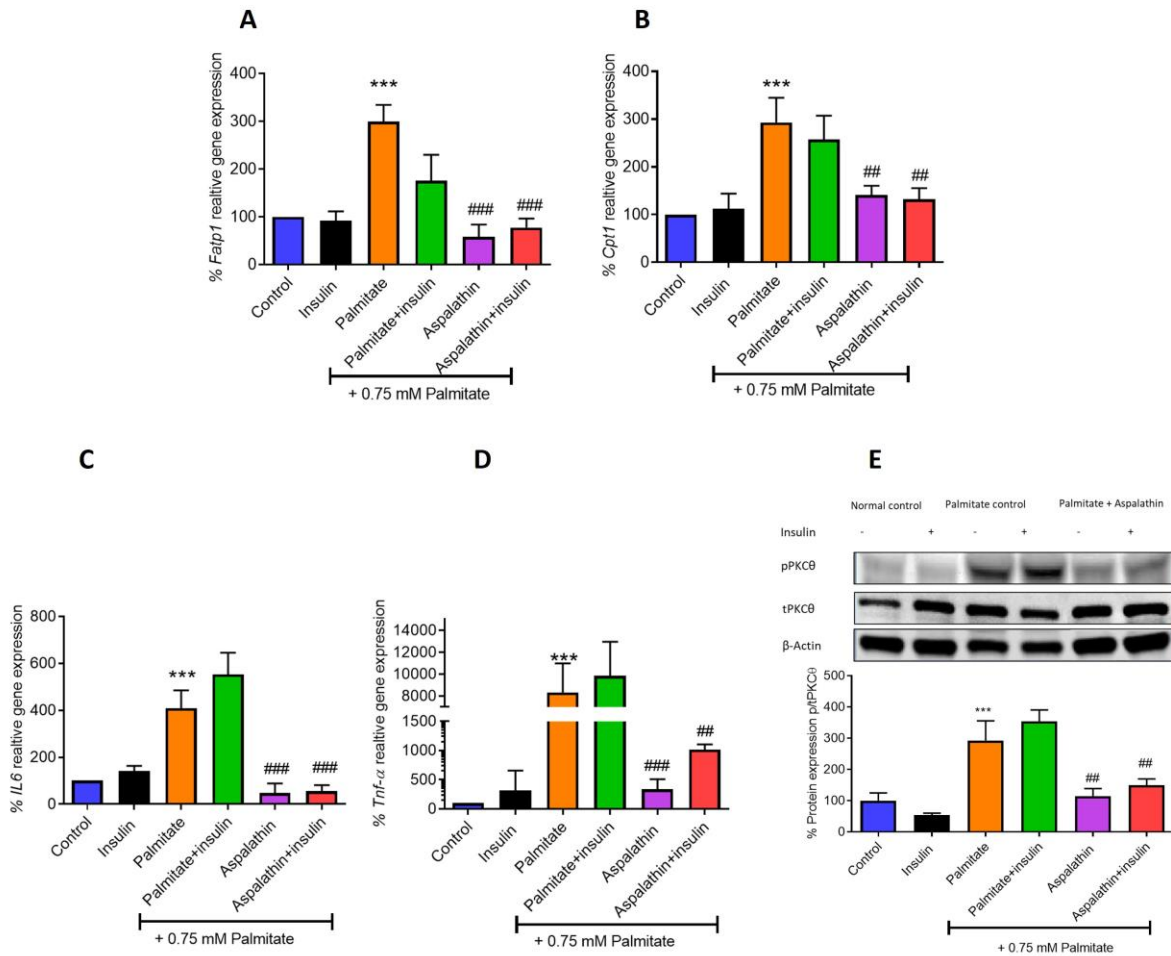
546

547



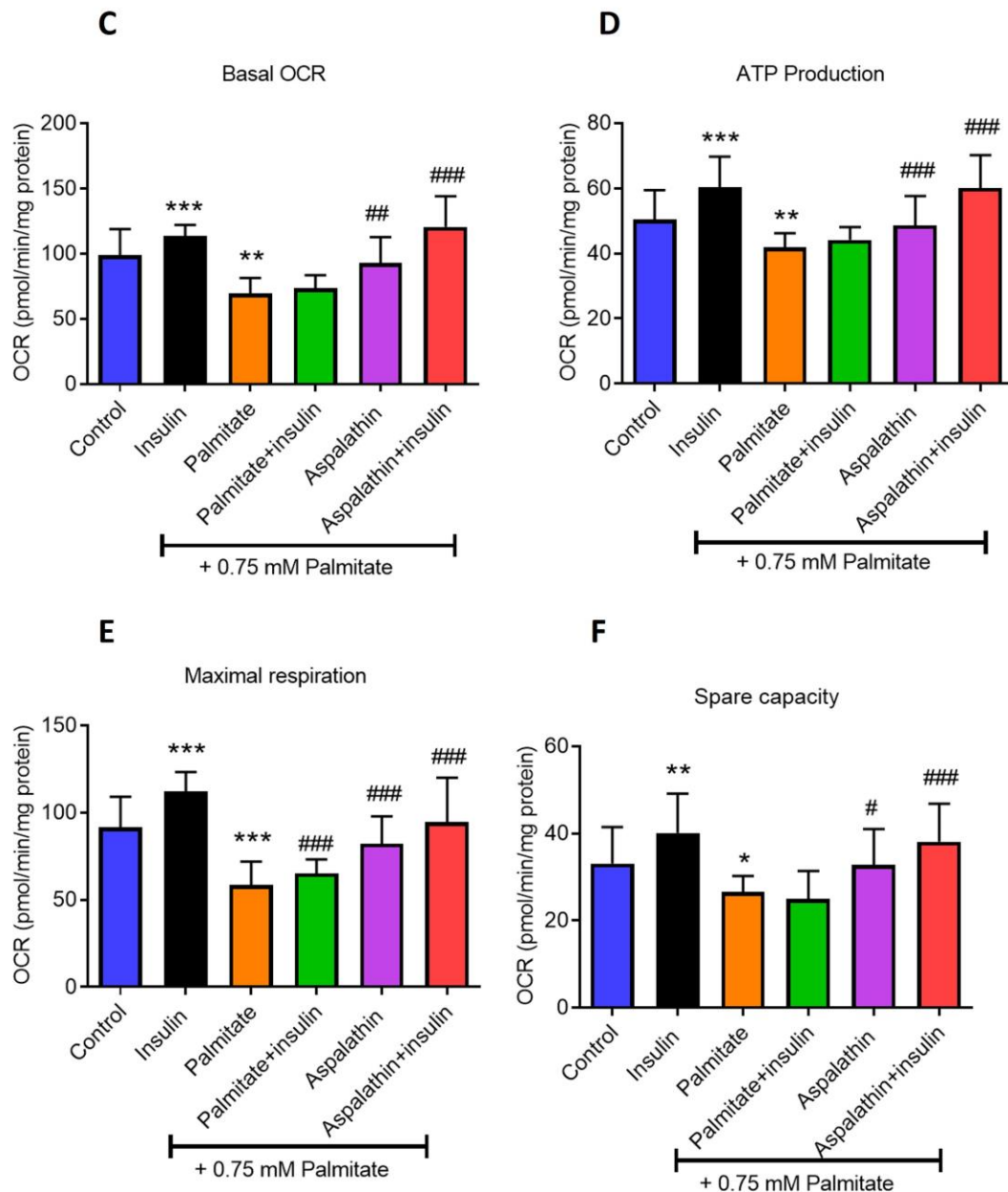
548

549 **Figure 2. Effect of aspalathin on glucose uptake (A), and protein expression levels of insulin receptor (IR; B), and**
 550 **phosphorylated protein kinase B (p/AKT; C) in insulin resistant skeletal muscle (C2C12) cells.** Briefly, C2C12 myotubules
 551 were treated with or without 0.75 mM palmitate for 16 h, thereafter cultured with aspalathin (10 μ M) for 1 h, while insulin
 552 (1 μ M) was added in the last 15 min as a positive control. Treated cells were lysed and subjected to Western blot analysis.
 553 Results are expressed as the mean of three independent experiments relative to control set at 100% \pm SEM ** p < 0.01, *** p <
 554 0.001 versus experimental control: ## p < 0.01, ### p < 0.001 versus palmitate control.



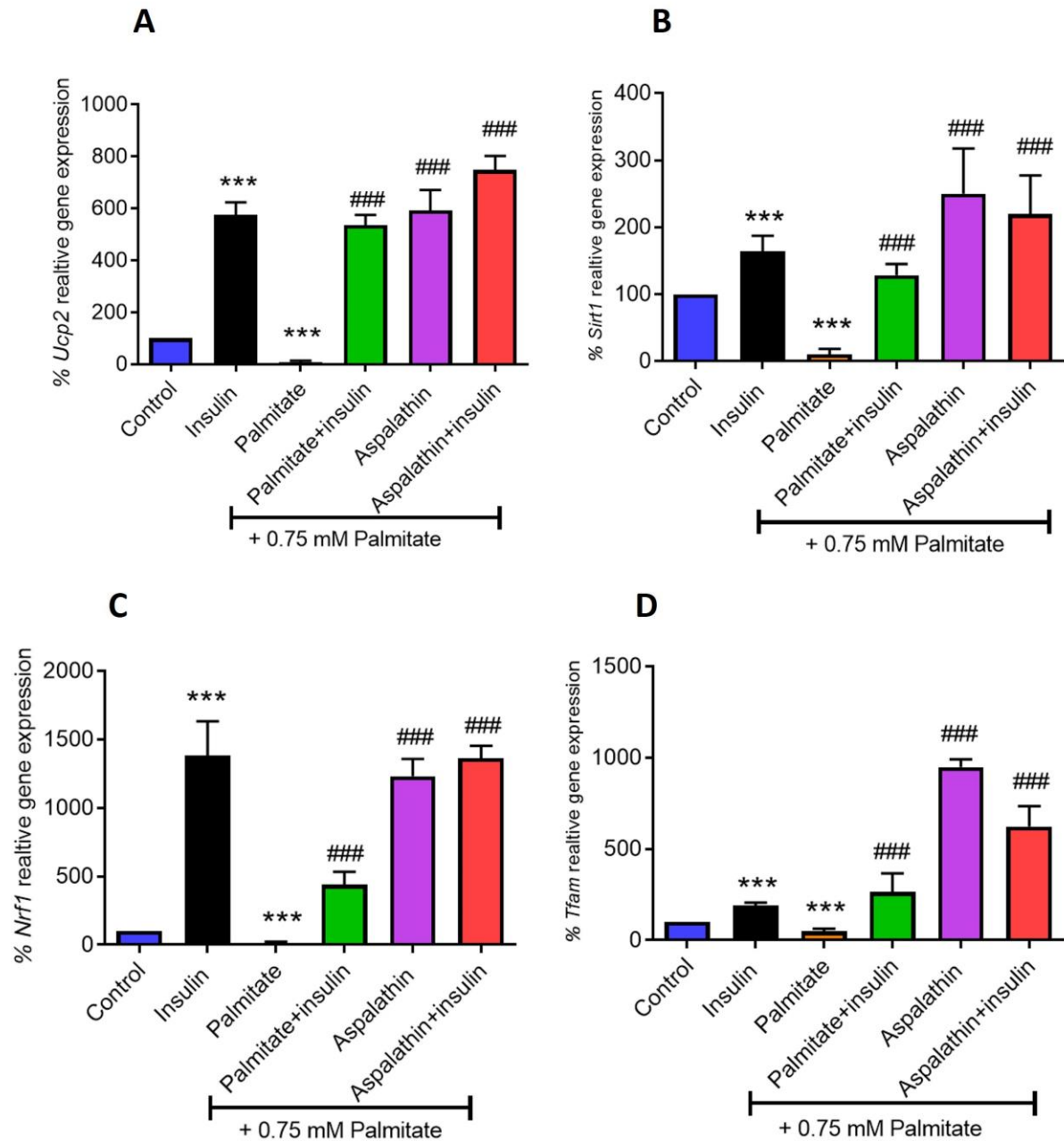
555

556 **Figure 3. Effect of aspalathin on the regulation of mRNA expression levels of genes involved in beta-oxidation like fatty**
 557 **acid transport protein 1 (Fatp1; A) carnitine palmitoyltransferase 1 (Cpt1; B), and genes involved in inflammation such as**
 558 **interleukin-6 (Il6; C) and tumor necrosis factor alpha (TNF-α; D), as well as protein expression of protein kinase C theta**
 559 **(PKC-θ; E) in insulin resistant skeletal muscle (C2C12) cells. Briefly, C2C12 myotubules were treated with or without 0.75 mM**
 560 **palmitate for 16 h, thereafter cultured with aspalathin (10 μM) for 1 h, while insulin (1 μM) was added in the last 15 min as**
 561 **a positive control. Treated cells were lysed and quantified by RT-PCR and protein analysis. Results are expressed as the mean**
 562 **of three independent experiments relative to control set at 100% ± SEM. ***p < 0.001 versus experimental control; ##p < 0.01,**
 563 **###p < 0.001 versus palmitate control.**



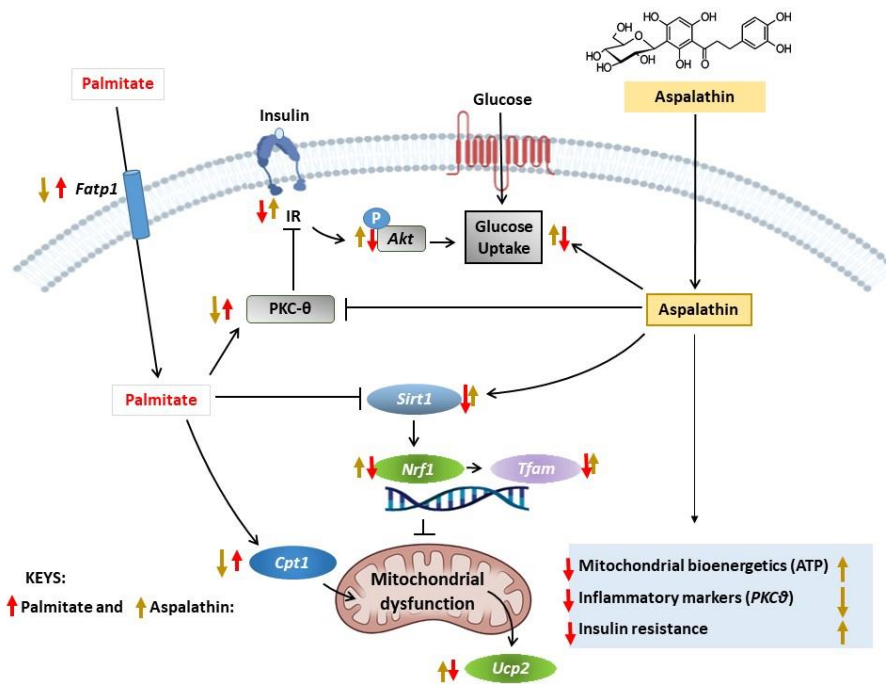
564

565 **Figure 4. Effect of aspalathin on the regulation of mitochondrial bioenergetics, including basal oxygen consumption rate**
 566 **(OCR; A) and extracellular acidification rates (ECAR; B) of all treatments, before independent analysis of basal OCR (C),**
 567 **adenosine triphosphate (ATP) production (D), maximal respiration (E), and spare respiratory capacity (F) in insulin resistant**
 568 **skeletal muscle (C2C12) cells. Briefly, C2C12 myotubules were treated with or without 0.75 mM palmitate for 16 h, thereafter**
 569 **cultured with aspalathin (10 μ M) for 1 h, while insulin (1 μ M) was added in the last 15 min as a positive control. The OCR and**
 570 **ECAR were determined using Seahorse XF-96 Metabolic Flux Analyzer. Groups (A, B, C, D, E and F) show data of changes in**
 571 **OCR, ECAR, in response to the sequential administration (arrows) of oligomycin (2 μ g/ mL) port A, Carbonyl cyanide-p-**
 572 **trifluoromethoxyphenylhydrazone (FCCP) (2.5 μ M) port B, antimycin and Rotenone (2.5 μ M) port C. Results are expressed as**
 573 **mean \pm SEM of 3 independent experiments. * $p \leq 0.05$, ** $p < 0.001$ *** $p < 0.001$ versus experimental control; # $p < 0.05$, ## $p <$**
 574 **0.05### $p < 0.001$ versus palmitate control.**



575

576 **Figure 5. Effect of aspalathin on the regulation of mRNA expression levels of genes involved mitochondrial function,**
 577 **including uncoupling protein 2 (Ucp2; A), silent mating type information regulation 2 homolog (Sirt1; B), nuclear**
 578 **respiratory factor 1 (Nrf1; C) and transcription factor A, mitochondrial (Tfam; D) in insulin resistant skeletal muscle (C2C12)**
 579 **cells. Briefly, C2C12 myotubules were treated with or without 0.75 mM palmitate for 16 h, thereafter cultured with aspalathin**
 580 **(10 μ M) for 1 h, while insulin (1 μ M) was added in the last 15 min as a positive control. Treated cells were lysed and quantified**
 581 **by RT-PCR analysis. Results are expressed as the mean of three independent experiments relative to control set at 100% \pm**
 582 **SEM. *** p < 0.001 versus experimental control: ### p < 0.001 versus palmitate control.**



583

584 **Figure 6:** An overview of therapeutic mechanisms by which aspalathin ameliorates palmitate-induced insulin resistance in
 585 skeletal muscle (C2C12) myotubules. Briefly, the major results in this study showed that aspalathin treatment could alleviate
 586 palmitate-induced skeletal muscle insulin resistance by enhancing glucose uptake and mitochondrial respiration blocking
 587 free fatty acid (FFA)-transport, as well as improving insulin signaling as partly demonstrated through increased expression
 588 insulin receptor (IR)/phosphorylation of protein kinase B (AKT) in cultured C2C12 myotubules. This bioactive compound could
 589 effectively attenuate inflammation by reducing the expression of markers such as interleukin-6 (*IL-6*), tumor necrosis factor-
 590 alpha (*TNF-α*), and protein kinase C-theta (PKC-θ). Moreover, markers of mitochondrial function included, included
 591 uncoupling protein 2 (*Ucp2*), NAD-dependent deacetylase sirtuin 1 (*Sirt1*), nuclear respiratory factor 1 (*Nrf1*) and
 592 transcription factor A, mitochondrial (*Tfam*).